 MCB, vol.3, no.3, pp.95-107, 2006

Intracellular Calcium Waves in Bone Cell Networks under Single Cell Nanoindentation

X. Edward Guo[*,†,‡], Erica Takai[*,‡], Xingyu Jiang[§], Qiaobing Xu[§], George M. Whitesides[§], James T. Yardley[¶], Clark T. Hung[*], Eugene M. Chow[‖], Thomas Hantschel[**], and Kevin D. Costa[*]

Abstract: In this study, bone cells were successfully cultured into a micropatterned network with dimensions close to that of *in vivo* osteocyte networks using microcontact printing and self-assembled monolyers (SAMs). The optimal geometric parameters for the formation of these networks were determined in terms of circle diameters and line widths. Bone cells patterned in these networks were also able to form gap junctions with each other, shown by immunofluorescent staining for the gap junction protein connexin 43, as well as the transfer of gap-junction permeable calcein-AM dye. We have demonstrated for the first time, that the intracellular calcium response of a single bone cell indented in this bone cell network, can be transmitted to neighboring bone cells through multiple calcium waves. Furthermore, the propagation of these calcium waves was diminished with increased cell separation distance. Thus, this study provides new experimental data that support the idea of osteocyte network memory of mechanical loading similar to memory in neural networks.

1 Introduction

Osteocytes are interconnected through numerous intercellular processes, forming extensive cell networks throughout the bone tissue (1, 2). Although it has been shown that osteocyte density is an important physiological parameter, with a decrease in osteocyte density with age and microdamage accumulation (3), most studies on osteocyte mechanotransduction have been performed on confluent or sub-confluent uncontrolled monolayers of bone cells (4-7). Also, a decrease in osteocyte connectivity and disruption of their spatial distribution has been observed in osteoporotic bone (8). Therefore, the ability to culture bone cells in a controlled network configuration, by modification of the surface chemistry, with prescribed cell separation distances and/or connectivity, would give insight into the response of bone cell networks to mechanical stimulation, in a scale that is more physiologically relevant than previously possible. Controlled bone cell culturing using micropatterning techniques, in combination with atomic force microscopy, which allows targeted stimulation of single cells within the network, would also provide a venue to study signal propagation between a single stimulated bone cell to neighboring bone cells in this controlled cell network.

In vivo, osteocyte bodies reside in lacunae approximately 10-15 μm in diameter, and connect to a maximum of 12 neighboring osteocytes through smaller channels (canaliculi) 0.2-0.8 μm in diameter and 15-50 μm long (9-11), in a 3-dimensional network. *In vitro*, bone cells generally exhibit high adhesion to many surfaces, and over time they can secrete their own extracellular matrix (ECM) proteins to modify the characteristics of the surfaces to which they adhere (12). Therefore, in order to micropattern bone cells in a 2-dimensional network with feature sizes that are close to that of canaliculi ($<$1 μm) and lacunae ($\sim$20 μm), well-controlled surface chemistry is necessary. Previously, bovine and human endothelial cells, hepatocytes, and fibroblasts have been successfully micropatterned using self-assembled monolayers (SAMs) and soft lithography techniques (microcontact printing), into lines as thin as 10 μm wide, and islands as small as 10 μm x 10 μm (13-17). SAMs spontaneously form ordered aggregates on metal-coated surfaces (*e.g.*, gold, platinum), and SAM modified surfaces

[*] Department of Biomedical Engineering, Columbia University, New York, NY 10027, U.S.A.
[†] Corresponding Author, E-mail: ed.guo@columbia.edu
[‡] These two authors contributed equally to this paper.
[§] Department of Chemistry and Chemical Biology, Harvard University, Cambridge, MA 02138, U.S.A.
[¶] Center for Electron Transport in Molecular Nanostructures, Department of Chemical Engineering, Columbia University, New York, NY 10027, U.S.A.
[‖] Palo Alto Research Center (PARC), 3333 Coyote Hill Road, Palo Alto, CA 94304, U.S.A.
[**] Interuniversity Microelectronics Center (IMEC), Kapeldreef 75, B-3001 Leuven, Belgium

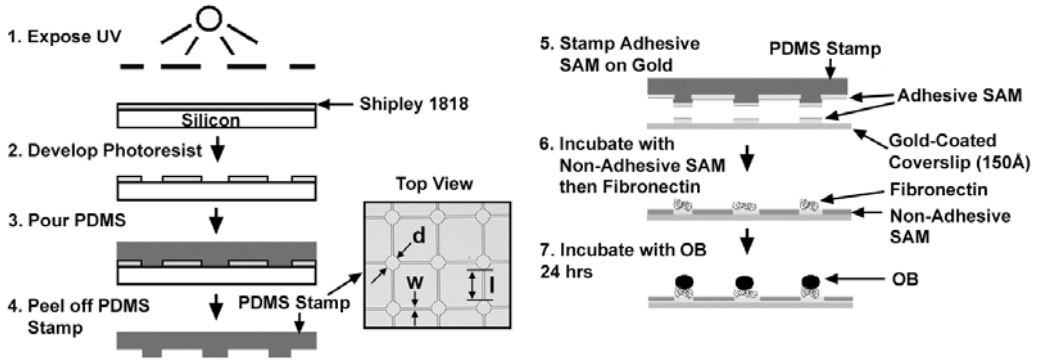

Figure 1 : Flowchart of PDMS stamp fabrication, microcontact printing, and cell patterning (OB=osteoblast). Inset is a top view photomicrograph of the PDMS stamp. Line width (w) of the patterns varies as 1, 2, or 3 μm, and circle diameter (d) varies as 10, 15, 20, or 25 μm, with a fixed separation distance (l) of 50 μm. Another similar stamp contained line widths fixed at 2 μm and circles of 15 or 20 μm diameter, with varied separation distances as 25, 50, or 75μm.

allow strict control of cell-surface interactions through the creation of micropatterns of ECM proteins, surrounded by non-adhesive SAM regions such that individual cells will attach and spread only to the ECM patterned adhesive regions. The micropatterning of SAMs can be accomplished either by microcontact printing using polydimethyl siloxane (PDMS) elastomeric stamps created using soft lithography (15-17), or by gold lift-off techniques (18, 19). In both techniques, alkanethiol SAMs can be micropatterned on gold coated surfaces, which have previously been used to control the interactions of surfaces with proteins (16, 20). Hydrophobic alkanethiol SAMs such as octadecanethiol (HS-$(CH_2)_{17}CH_3$) rapidly and irreversibly adsorb proteins and promote cell adhesion, while SAMs that present ethylene glycol moieties such as tris-(ethylene glycol)-terminated alkanethiols (HS-$(CH_2)_{11}(OCH_2CH_2)_3$OH) effectively resist protein absorption and cell adhesion (15, 17, 18, 20-23). Thus, the patterning of these two SAMs on a substrate defines the pattern of ECM proteins that are adsorbed from solution onto the substrate, and a grid of adhesive ECM islands and lines limits cell attachment to those islands. Although other modified silanes have been used to pattern bone cells (18, 24) into relatively thick lines or islands (several cells wide), alkanethiol SAMs have not been previously used to pattern bone cells, and bone cells have never been cultured in network patterns that closely mimic osteocyte networks *in vivo*.

The goals of this study were to 1) optimize the geometric parameters to create bone cell networks, 2) examine calcium wave propagation from a single bone cell nanoindented using an atomic force microscope to neighboring cells in this bone cell network, and 3) examine the effect of separation distance on calcium signal propagation.

2 Materials and Methods

2.1 Microcontact Printing for the Formation of Controlled Bone Cell Networks

Fibronectin (FN) patterns were created on gold-coated coverslips using microcontact printing techniques with SAMs and a PDMS elastomeric stamp, in a similar manner to Chen *et al.*, (15). Briefly, a mold was fabricated using Shipley 1818 positive photoresist (MicroChem Corp, Newton, MA) by spin-coating a 2 μm thick film of photoresist onto silicon wafers and exposing the photoresist to UV light through a chromium mask containing the desired grid and circle features (Fig. 1). The photoresist was then developed in a commercial Shipley photoresist developer, and exposed to a vapor of (tridecafluoro 1,1,2,2 tetrahydro octyl)-1-trichlorosilane to facilitate easy removal of the PDMS from the master. A 10:1 mixture of PDMS pre-polymer and curing agent (Sylgard 184 kit, Dow Corning, Midland, MI) was then prepared, poured onto the master, and placed under a vacuum to evacuate all air bubbles. The PDMS mixture was then cured at 70^{o}C for 2-4 hours and removed from the master such that the PDMS stamp contained the raised circle

and grid micropatterns (Fig. 1 inset). To initially determine the optimal geometric parameters for network pattern formation, a mask with line widths varied as 1, 2, or 3 μm and circle diameters ranged as 10, 15, 20, or 25 μm, with a fixed cell separation distance of 50 μm was used. Then to examine the effects of separation distance on signal propagation, another mask containing lines of 2 μm width and circles of 15 or 20 μm in diameter, with varying separation distances of 25, 50, or 75 μm, was used.

Coverslips 48x65 mm were coated with a 10-15 Å adhesion layer of titanium and $\sim$150 Å of gold using an electron-beam evaporator (Semicore SC200; Livermore, CA). The PDMS stamp was then coated with octadecanethiol (adhesive SAM; Sigma-Aldrich Co., St. Louis, MO), which allows cell adhesion, dried for 30 seconds under a gentle stream of nitrogen, and pressed onto the gold coverslips for 60 seconds (Fig. 1). The stamped coverslips were then immersed in an ethylene glycol terminated SAM solution ($HS\text{-}C_{11}\text{-}EG_3$, non-adhesive SAM; Prochimia, Sopot, Poland) for 1-3 hours to prevent cell adhesion to areas that were not patterned with the adhesive SAM. The patterned coverslips were then rinsed, dried under nitrogen, and further incubated with a 10 μg/ml solution of fibronectin (FN, Invitrogen, Carlsbad, CA), which was only absorbed to the adhesive SAM patterned regions. Osteoblast-like MC3T3-E1 cells were then seeded on these patterned coverslips at a density of $1.0\text{x}10^4$ cell/cm^2 and cultured in α-minimum essential medium (α-MEM) supplemented with 2% charcoal-stripped fetal bovine serum (CS-FBS; Hyclone Laboratories Inc., Logan, UT) and allowed to migrate onto patterns for 24 hours.

2.2 Optimization of Geometric Parameters for Bone Cell Network Formation

To confirm good micropatterning, coverslips patterned with FN but not seeded with cells were subjected to immunofluorescent staining for FN using an anti-FN primary antibody (Chemicon, Temecula, CA) and a FITC conjugated secondary antibody (ICN/Cappel, Aurora, OH). Images of the stained coverslips were obtained using an inverted fluorescence microscope (Olympus IX-70, Melville, NY) with a 40x objective. Also, to confirm proper fabrication of the stamp features, the nominal features of stamps with a fixed 50 μm separation and variable line widths and circle diameters were measured 3 times and averaged from images obtained using a light microscope and Scion Image (Frederick, MD), image analysis software.

To determine the most optimal line widths and circle diameter sizes for the formation of bone cell networks, MC3T3-E1 cells were patterned as described above using stamps with a fixed separation distance of 50 μm, then fixed in 10% buffered formalin, and subjected to immunofluorescent staining against fibronectin and counterstained with a propidium iodide nucleic acid counterstain (Molecular Probes, Eugene, OR). An area 15x15 cells in the center of the patterned regions was analyzed. The total number of cells in the correct place (nucleus/cell body in the circle regions) and incorrect place were manually counted to give the fraction of cells in the correct place/cells in the incorrect place. To assess connectivity, the number of nodes and branches were counted manually, and connectivity was defined to be $\chi = \varepsilon/\text{nodes}$, where ε is the Euler number which is defined as ε = number of nodes – number of branches (25). The Euler number was divided by the number of nodes in the analyzed area in order to obtain a connectivity measure that is independent of sample area size. The ideal connectivity for a network of 4 adjacent neighbors is -1.

2.3 Assessment of Gap Junction Formation

Immunofluorescent staining against connexin 43 (Cx43) was performed on bone cells patterned as described above, which were then fixed with cold acetone for 20 minutes at -20 $^\circ$C. To visualize gap junctions, the osteoblasts on the patterned glass coverslips were incubated with a polyclonal anti-Cx43 (Chemicon) primary antibody followed with a FITC-conjugated anti-rabbit (Molecular Probes) secondary antibody, then counterstained with propidium iodide nucleic acid counterstain. Samples were then examined using a fluorescence microscope with a 60x objective lens.

To assess the formation of functional gap junctions, a technique employing calcein dye transfer from fluorescently double labeled cells was used (7, 26). Bone cells were trypsinized and stained with 5μM 1,1' -dioctadecyl-3,3,3' ,3' -tetramethylindocarbocyanine perchlorate (DiI, Molecular Probes) for 20 minutes, followed by 4 μM calcein acetoxymethyl ester (calcein-AM, Molecular Probes) for 30 minutes. DiI is a membrane-bound dye that will not transfer to neighboring cells, thus serving as an indicator of the original double la-

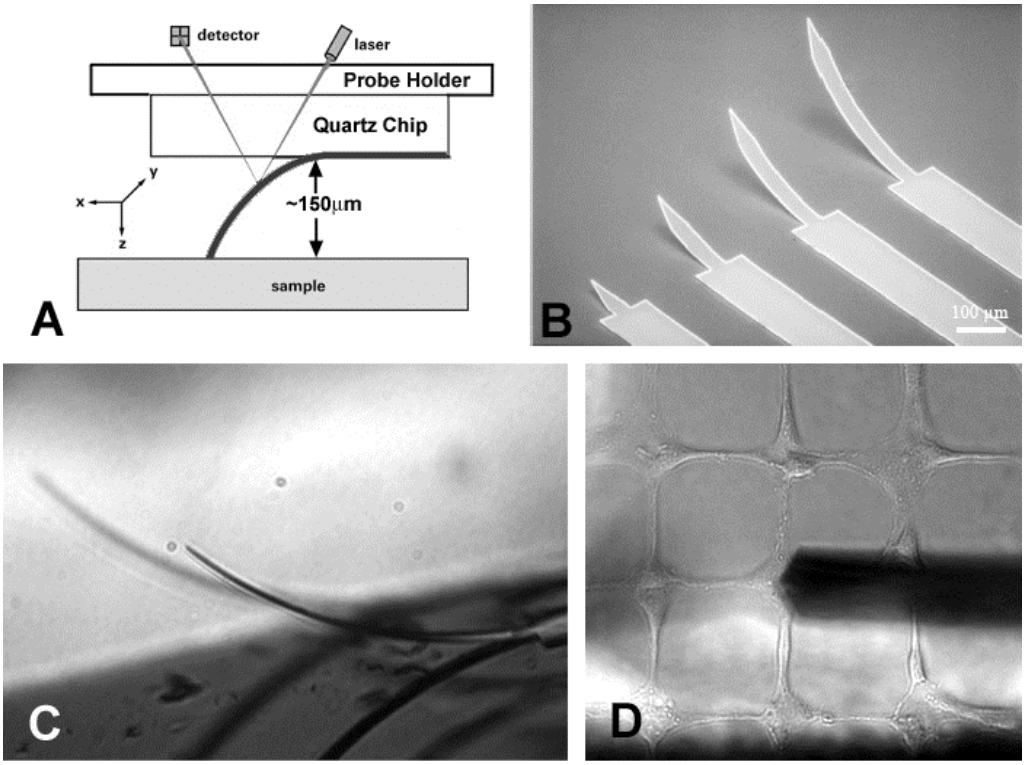

Figure 2 : StressedMetal^{TM}probe. A) Side-view illustration of the longest probe indenting a sample; B) SEM image of probes; C) Side view light micrograph of longest and second longest probes; D) Top view light micrograph of the longest probe indenting a single bone cell in the network. A and B are adopted from www.parc.com.

beled cells, while calcein is a gap junction permeable dye. The double labeled cells were then mixed with a suspension of unlabeled bone cells at a ratio of 1:80 and cultured on the fibronectin patterned coverslips as described above. After culturing the cells overnight, the patterned cells were imaged using a fluorescent microscope equipped with a rhodamine filter (red) to visualize the original double labeled cells, and a fluorescein filter (green) to visualize neighboring cells that received the calcein dye through gap junctional coupling to the double labeled cells.

2.4 Single-Cell Nanoindentation Using Atomic Force Microscopy

To examine the effects of cell separation distance on calcium wave propagation from a single indented bone cell, bone cells were cultured into patterns with 20 μm or 15 μm diameter circles and 2 μm wide lines, with a separation distance of 50, or 75 μm, according to the procedures described above. Patterned cells were loaded with Fluo-4 AM (Molecular Probes, Eugene, OR), a fluorescent calcium indicator dye, by incubating the cells in a solution containing 5 μM Fluo-4 AM, 0.02% pluronic F-127 for even dispersion of the dye, and α-MEM supplemented with 0.5% CS-FBS, for 2 hours at room temperature. The glass coverslips containing the patterned bone cells were then placed under an atomic force microscope (AFM; Bioscope, Digital Instruments/Veeco, Santa Barbara, CA) mounted on an inverted fluorescence microscope (Olympus IX-70) equipped with a cooled digital CCD camera (Sensicam, Cooke Corp, Auburn Hills, MI), and allowed to equilibrate to ambient conditions for $\sim$5 minutes. The AFM was mounted with a specialized probe with an extremely high aspect ratio (StressedMetal^{TM}, Palo Alto Research Center, Palo Alto, CA), $\sim$150 μm high x 400 μm long, to minimize fluid motion at the cell surface due to the probe holder displacement (Fig. 2) (27, 28). The stiffness of the probe was 0.06 N/m (29). These stress-engineered cantilever probes are unique because they are much taller than conventional probes and fabricated on optically transparent substrates, which enables straightforward measurements

Table 1 : Nominal dimensions of the PDMS stamps and percent error of nominal dimensions from the prescribed dimensions.

	Prescribed Dimension	Nominal Dimension	Standard Deviation	Percent Error
Line Width (μm)	1	0.99	0.1	-0.7
	2	1.80	0.2	-10.0
	3	2.46	0.3	-18.1
Circle Diameter (μm)	10	10.17	0.3	+1.7
	15	14.79	0.2	-1.4
	20	19.59	0.3	-2.0
	25	24.50	0.4	-2.0

inside fluids because the fluid is flush against the glass. In addition, the stress-engineered cantilever tips can be hundreds of microns away from the AFM probe holder and parallel to the sample substrate. In contrast conventional cantilevers are only tens of microns tall and require angled operation that complicates optical detection for the StressedMetal probe. A custom probe holder was made such that the StressedMetal probe was held at a 0° angle with the contact surface, rather than the 12° angle of conventional probe holders, to optimize the reflection of the laser spot on the probe. A single bone cell in the network pattern was stimulated by continuous indentation at 1 Hz, in relative trigger mode, to apply a prescribed contact force of 61.6 ± 13 nN, which resulted in an 823 ± 380 nm indentation depth (locally). The AFM nano-indentation experiment involves monitoring the deflection of the StressedMetal probe as its tip contacts and indents the cell. The resulting interaction force bends the probe, which is detected by the movement of a reflected laser spot.

Simultaneously with the nano-indentation, fluorescence time-lapsed images of intracellular calcium ($[Ca^{2+}]_i$) waves in bone cells were taken every 2 seconds, starting 60 seconds prior to stimulation, to obtain baseline $[Ca^{2+}]_i$ levels, to up to 5 minutes after the start of the stimulation. Images were analyzed using Metamorph 4.1^{TM} imaging software (Universal Imaging Corp., West Chester PA), where the mean fluorescence intensities of individual cells were measured and background fluorescence was subtracted for each time-lapsed image. The relative change in intracellular calcium was determined by dividing the fluorescence measurement of each cell after stimulation by the average baseline fluorescent intensities of each cell prior to stimulation. The response of individual bone cells in a field of view, using a 20x objective, was analyzed, thereby permitting the analysis of individual cell responses. A responsive cell was defined as a cell with a calcium oscillation of at least four times the maximum oscillation measured during the baseline measurement period immediately before stimulation (30). The speed of calcium wave transmission was also determined by dividing the distance between the nano-indented cell and neighboring responding cells by the time between the response of the nano-indented cell and neighboring responding cells. The percentage of responding cells immediately adjacent and two cells away, were also determined. Five experiments were performed for each separation distance, with a total of 30 and 24 responding cells analyzed in cell networks with 50 and 75 μm separation distances, respectively. The calcium signal transmission speed from the indented bone cell to neighboring bone cells of various cell steps (*e.g.*, one cell away, two cells away) and differences in the percentage of responding cells with each cell step at different separation distances was compared. The peak calcium response magnitudes of cells, between different separation distances at each cell step were also analyzed. To determine statistical significance between different conditions a two-way ANOVA with a Fisher's post-hoc analysis (Systat, Point Richmond, CA) was used. For all statistical analyses a p value of less than 0.05 was considered significant.

3 Results

3.1 Assessment of Cell Patterning

Measurements of the PDMS stamp features using Scion Image showed that the nominal dimensions of the fabricated stamps were slightly smaller than the prescribed feature dimensions by a maximum of 18.1% for line widths and 2.0% for circle diameters (Table 1). Variations in the nominal dimensions were due to slight alterations in photoresist thickness, PDMS shrinkage, or UV

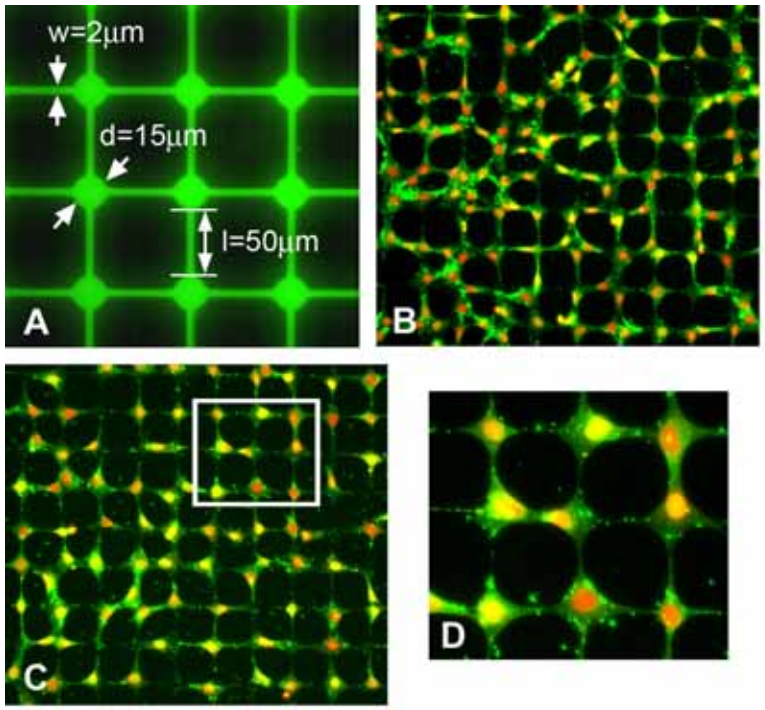

Figure 3 : A) Fluorescence micrograph of a typical micropatterned coverslip stained against fibronectin. Micropatterned features of other dimensions were similar. B-D) Micropatterned bone cells stained with fibronectin (green) and propidium iodide nuclear counterstain (red). B) Least optimal pattern with w=3 μm x d=25 μm. C) Optimal pattern w=2 μm x d=20 μm; D) enlargement of C) illustrating that cell bodies reside in circles and processes extend along lines.

Table 2 : Quantitative assessment of bone cell pattern formation with varying feature dimensions. The ideal connectivity for a network of 4 adjacent neighbors is -1.

Dimensions	%Correct of Total Cells	Correct/Incorrect	Euler #	Connectivity
1μmx10μm	76.0	3.5	-193.3	-1.34
1μmx15μm	78.9	3.8	-184.2	-1.47
1μmx20μm	73.1	3.0	-233.7	-1.46
1μmx25μm	72.2	3.2	-242.3	-1.38
2μmx10μm	82.5	4.7	-212.7	-1.40
2μmx15μm	83.0	4.9	-190.3	-1.32
2μmx20μm	81.6	4.5	-195.2	-1.20
2μmx25μm	77.4	3.5	-205.8	-1.28
3μmx10μm	74.8	3.2	-226.2	-1.24
3μmx15μm	81.2	4.9	-200.8	-1.18
3μmx20μm	58.4	1.4	-326.2	-1.56
3μmx25μm	68.1	2.8	-239.8	-1.34

exposure time. Fluorescence micrographs of patterned coverslips stained for fibronectin showed consistent good pattern transfer for all feature dimensions (Fig. 3). Transferred pattern dimensions were larger than the nominal stamp dimensions by a maximum 27.2% for line widths and 28.8% for circle diameters.

Qualitatively, good pattern formation was achieved, where the majority of cell bodies reside in the circles and the cell processes extend along the lines (Fig. 3). Quantitative assessment of pattern formation revealed that, in general, features with 2 μm wide lines had the highest fraction of cells in correct/incorrect locations, while w=2

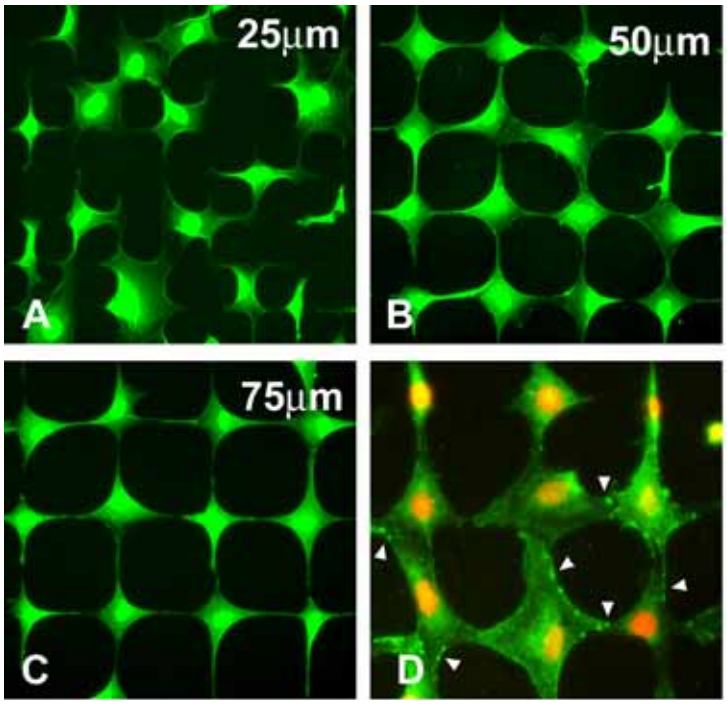

Figure 4 : A-C) Micropatterned bone cells with 25, 50, or 75 μm intercellular separation distances stained with eosin (green). 50 and 75 μm separation distances support good pattern formation, while a 25 μm separation allows bone cells to span multiple spots. D) Connexin 43 (Cx43) staining (green) and propidium iodide nucleic acid counterstain (red). Arrowheads show areas of high punctate Cx43 staining between adjacent cells, suggesting gap junction formation.

μm x d=20 μm and w=3 μm x d=15 μm showed the best connectivity (Table 2). In contrast, larger circle diameters and larger line widths (w=3 μm x d=20-25 μm) led to least optimal patterning with many cells adhering to the line areas, and significantly lower correct/incorrect cell positioning ratios. For patterns with varying separation distances, bone cells could only be successfully cultured into network patterns at 50 and 75 μm separation distances but not 25 μm separation distance, since this shorter distance allowed cell bodies to span over multiple circles, thus preventing good network pattern formation (Fig. 4).

Immunofluorescence staining for Cx43 gap junction protein showed punctate Cx43 staining at the ends of cell processes, which suggests that gap junctions were formed between cells in the micropatterned bone cell network (Fig. 4D). The calcein dye transfer assay showed that neighboring cells at least 1 to 2 cell steps away from the original double labeled cells were able to receive the calcein dye, demonstrating that functional gap junctions form between bone cells in the network patterns (Fig. 5). The calcein dye transfer was similar in bone cell networks with 50 and 75 μm separation distances.

3.2 Calcium Wave Propagation in Bone Cell Networks

Intracellular calcium signals were observed to propagate from a single stimulated bone cell (cell #1) to adjacent cells micropatterned in the network configuration at both 50 and 75μm separation distances (Fig. 6). Some neighboring cells (#3 and #5) were able to respond with a second calcium transient through different cell paths. For example, cell #3 first showed a response propagated through cell #2, then a second response through cells # 6 and # 7. Similarly, cell #5 responded first through the indented cell (#1), then responded for a second time through cells #6 and #9. The magnitudes of the second calcium transient of cells #3 and #5 were similar to the magnitudes of the first responses (Fig. 7), and in general, second responses were not smaller than the first responses in networks with 50 μm separation distances (Fig. 8). The second responses in networks with a 75 μm

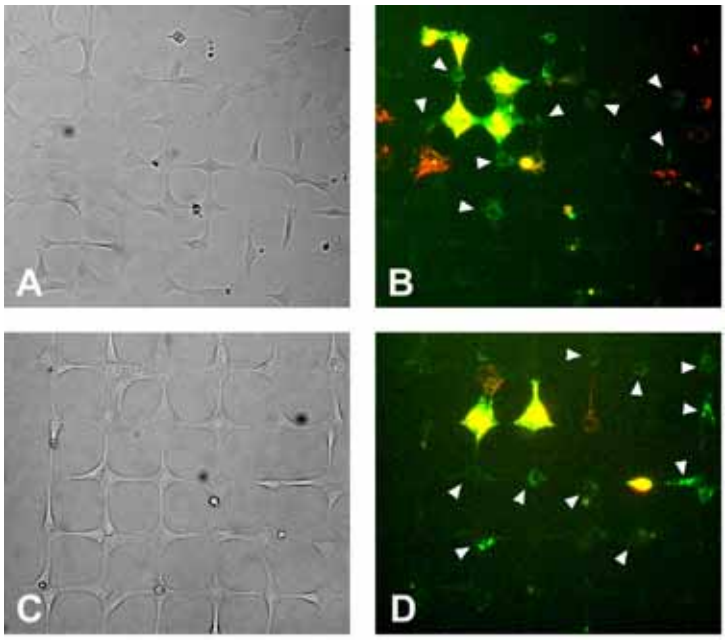

Figure 5 : Calcein dye transfer assay to assess functional gap junction formation. Panels A and C are light micrographs, and B and D are fluorescence micrographs. A, B) 50μm separation distance. C, D) 75 μm separation distance. Calcein dye (green, arrowheads) was transferred to neighboring cells at least 2 cell steps away from the original double labeled cells (red/yellow) in both bone cell networks of 50 and 75 μm separation distance.

separation were smaller than the first responses. An average of 73.3$\pm$5 and 105.0$\pm$51 seconds elapsed between first and second responses for 50 μm (n=3) and 75 μm (n=2) separation distances, respectively.

There was no significant difference in transmission speed with increased cell steps (1 *vs.* 2 cells away) or with increased separation distance (50 *vs.* 75 μm) (Fig. 9). The mean transmission speeds were 3.7$\pm$2.8 and 3.3$\pm$2.3 μm/sec for 50 and 75 μm separation distances, respectively. In addition, the magnitudes of the calcium responses of neighboring cells were significantly smaller than that of the indented cell (Fig. 9). However, there was no significant difference between the response magnitudes of cells 1 step or 2 steps away for either separation distance. There was a significantly smaller percentage of responsive cells 2 cell steps away in networks with a 75 μm separation distance compared to those with a 50 μm separation distance (Fig. 10). However, there was no difference in the percentage of responsive cells 1 cell step away, or directly adjacent to the indented bone cell, regardless of the cell separation distance.

4 Discussion

In this study, bone cells were successfully cultured into a micropatterned network with dimensions close to that of *in vivo* osteocyte networks. The optimal geometric parameters for the formation of these networks were determined in terms of circle diameters and line widths. Bone cells patterned in these networks were also able to form gap junctions with each other, shown by immunofluorescent staining for the gap junction protein connexin 43, and transfer of the gap junction permeable calcein dye. Furthermore, we have demonstrated for the first time, that the intracellular calcium response of a single bone cell indented in this bone cell network, can be transmitted to neighboring bone cells through multiple calcium waves.

The formation of neural network circuits in the brain is the key to permanent memory in cognitive functions (31). Osteocytes in mineralized bone tissue also form elaborate cellular networks. It is well known that mechanical usage modulates the shape, mass, and microstructure of bone. Does the osteocyte network hold the key to cellular memory of mechanical loading history in bone tissue? This is an interesting hypothesis which may have a pro-

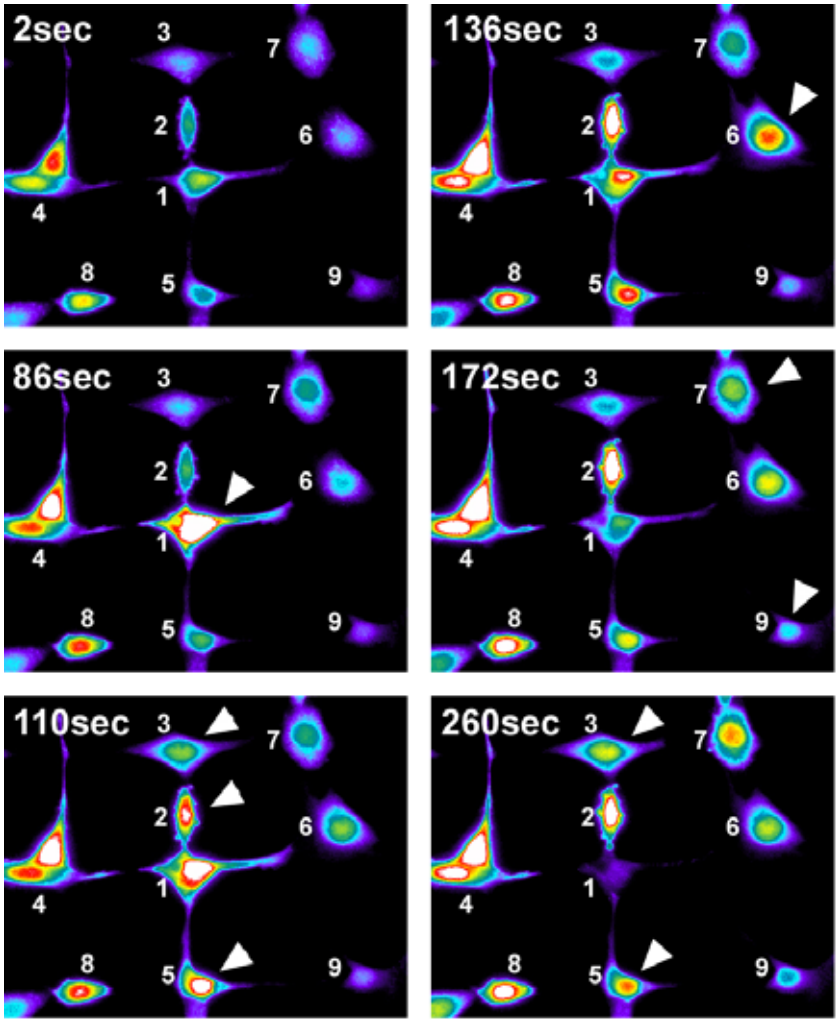

Figure 6 : Calcium signal propagation from a single indented bone cell (#1) to adjacent cells in the network pattern with a 50 μm separation distance. Arrowheads highlight some responding cells. Cells #3 and #5 were able to respond twice through different cell pathways.

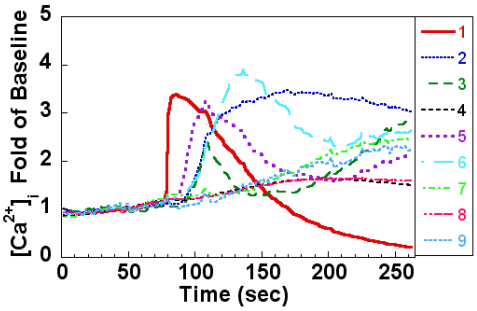

Figure 7 : Calcium response expressed as the fold change in $[Ca^{2+}]_i$ over baseline over time, corresponding to the cells in Figure 6. Cell #1 is the indented cell.

found implication in cellular and molecular mechanisms of bone adaptation to mechanical loading (32). The current study (with osteoblast-like cells) may be suggestive of the potential for osteocyte network memory of mechanical loading reminiscent of neural networks.

The PDMS stamps were successfully fabricated with actual dimensions similar to the prescribed feature specifications. The dimensions of the patterned fibronectin were up to 29% larger than the stamp dimensions, and this enlargement may in part be due to lateral expansion of the raised stamp features due to the weight of the stamp. There may also be some systematic overestimation of patterned feature measurements due the difficulty in determining the edges of the fibronectin pat-

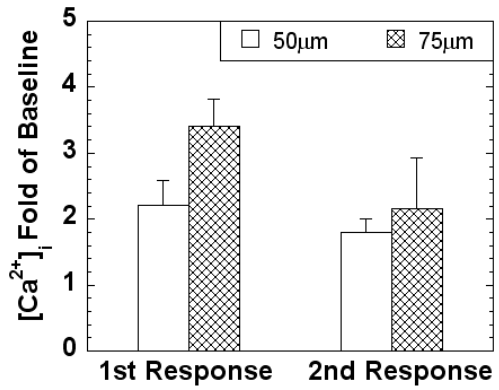

Figure 8 : Magnitude of 1^{st} and 2^{nd} calcium responses expressed as a fold increase over baseline calcium measurements, for bone cells networks with 50 and 75 μm separation distances. n=3 for 50 μm and n=2 for 75 μm separation distance networks. Results are expressed as means $\pm$ standard deviations.

terned features, which had a faint halo of fluorescence along the edges. Thus the actual pattern feature dimensions that promote optimal pattern formation are slightly larger than 15 or 20 μm circles x 2 μm wide lines.

Intracellular calcium transients were observed to be propagated from an indented bone cell to neighboring bone cells, both in networks with 50 and 75 μm separation distances. Some bone cells were able to exhibit double responses in intracellular calcium through signal propagation from two different cell paths. The time delay between the first and second responses ranged from approximately 65 to 150 seconds apart, similar to a previous finding that approximately 60-600 seconds elapsed between consecutive calcium responses of bone cells subjected to constant oscillatory fluid shear (30). The time between responses were similar for both bone cells patterned with 50 and 75 μm separation distances. However, bone cells responding multiple times to fluid shear were shown to have decreased magnitude of subsequent responses compared to the initial response, while in the current study, second responses of bone cells were similar in magnitude to that of the first response. It is important to note that in the fluid shear study performed by Donahue *et al.*, all of the bone cells were stimulated with fluid shear, while in the current study the cells exhibiting second responses were not directly mechanically stimulated. Therefore, it is possible that the behavior of the calcium response differs between direct cell response to mechanical stimulation and propagated responses. Out of 10 experiments total, we were able to observe cells with multiple responses in 5 experiments (50%). The ability of bone cells to respond multiple times, without a decrease in the magnitude of the calcium response to transmitted calcium waves may play a role in memory of bone cell networks of their previous mechanical loading history. This mechanism may also have similarities with memory in neural networks (33, 34). Thus, it would be of interest to examine whether there is an increase in gap junctional connections between bone cells along cell pathways with multiple responses in the network after mechanical stimulation. It is also possible that the multiple response behavior of bone cells in these networks modulate the signaling between osteocytic networks and osteoblasts on the surface of the bone.

The mean signal transmission speeds of 3.7 ± 2.8 for 50 μm and 3.3 ± 2.3 μm/sec for 75 μm separation distances measured in this study were similar to the signal transmission speed of $\sim$2.5 μm/sec and $\sim$0.5 μm/sec in osteoblasts (ROS 17/2.8) cultured in uncontrolled monolayers (35, 36). Furthermore, the finding that signal propagation speed does not diminish with increased number of cell steps away from the indented bone cell, is in agreement with previous the findings of Xia and Ferrier (35), and suggests that the calcium signal may be regenerated to a certain extent at each cell. Also, even with increased cell separation distance from 50 to 75 μm, the signal transmission speed was not significantly reduced, supporting the idea that the signal transmission is not due to diffusion of secreted factors. Interestingly, a previous study of osteoblasts in nearly confluent monolayers showed that transmission of calcium signals through secretion of paracrine factors such as ATP is faster, with a transmission velocity of $\sim$10 μm/sec, compared to gap junctional communication, with a transmission velocity of $\sim$0.5 μm/sec (36).

The peak magnitudes of calcium responses in neighboring cells were significantly lower than that of the indented cell. However, the peak magnitudes were not decreased with transmission between other neighboring cells, such as cells 1 step away and 2 steps away. One possible explanation is that the mechanism of the calcium response between the indented cell and the neighboring non-indented cells may be different. Specifically, the calcium response of the indented cell may be through influx of external calcium, while the responses of non-

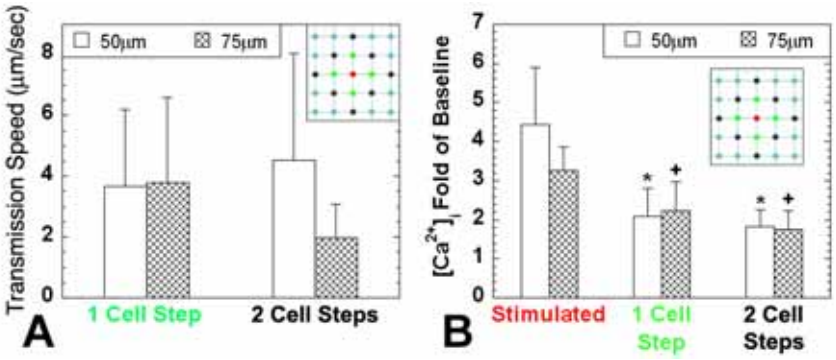

Figure 9 : A) Transmission speed of calcium signal from the indented bone cell to bone cells 1 cell step and 2 cell steps away, in bone cell networks with separation distances of 50 μm or 75 μm. Inset: red = indented cell, green = 1 cell step away, black = 2 cell steps away. There is no significant change in transmission speed regardless of the number of cell steps or separation distances. B) Magnitude of the peak calcium response with each progressive cell step expressed as a fold increase over baseline calcium measurements. There is a significant decrease in calcium response between the indented cell and cells 1 or 2 steps away. *p$\leq$0.001 with stimulated cell in 50 μm separation distance network; $^{+}$p$\leq$0.01 with stimulated cell in 75 μm separation distance network. There is no significant difference between the response magnitudes of cells 1 step or 2 steps away for either separation distance. Results are expressed as means $\pm$ standard deviations.

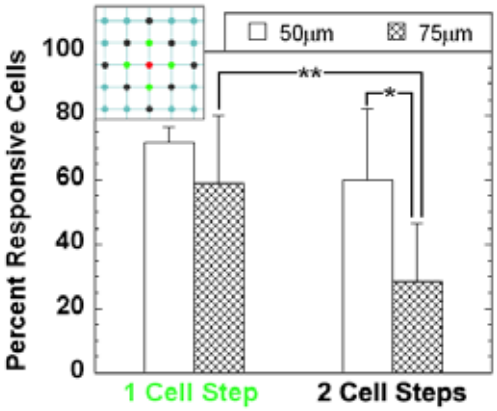

Figure 10 : Percentage of responsive bone cells 1 cell step and 2 cell steps away, in bone cell networks with separation distances of 50 μm or 75 μm. Inset: red = indented cell, green = 1 cell step away, black = 2 cell steps away. There is a significantly smaller percentage of responsive cells 2 cell steps away in networks with a 75 μm separation distance compared to those with a 50 μm separation; *p=0.02. There was also a significant decrease in the percentage of responsive cells between 1 cell step and 2 cell steps away, in bone cell networks with a 75 μm separation distance; **p=0.01. Results are expressed as means $\pm$ standard deviations. n=5 experiments.

indented cells may be dependent on the release of internal calcium stores. In support of this idea, previous studies using UMR 106-01 and HOBIT osteoblastic cells in uncontrolled monolayers have shown that depletion of internal calcium stores did not effect cell response to mechanical perturbation with a micropipette, but abolished the propagation of calcium response to neighboring cells (36, 37). In contrast, removal of external calcium decreased the mechanical response of the indented cell but did not effect calcium signal propagation to neighboring cells (37).

Although the transmission speeds of calcium signals and the magnitudes of responses were not significantly different between bone cells in networks with 50 or 75 μm separation distances, the percentage of responsive cells 2 cell steps away was significantly lower in networks with 75 μm separation distance. It has been previously proposed that bone cell response to mechanical stimulation (fluid shear) of different magnitudes may be encoded by the percentage of responsive cells, where the percentage of responsive cells at any calcium response magnitude threshold increases with the magnitude of stimulation (38). Thus, signaling within osteocytic networks and to osteoblasts may also be dependent on the percentage of responsive cells. Reduced osteocyte density in aged, microdamaged, or osteoporotic bone (3, 8, 39, 40) increases

separation distances between osteocytes, and may diminish the percentage of responsive cells to mechanical loading of bone, thereby reducing the signaling to other bone cells on the surface. The reduction in bone cell signaling with increased cell separation distance or decreased cell density may explain the reduced mechanosensitivity of bone with age (41, 42).

For future studies, it would be necessary to repeat this study on osteocytes and to examine the interaction between the osteocyte network and osteoblasts. It would also be interesting to examine calcium propagation responses of bone cell networks subjected to different magnitudes of mechanical stimulation. Since the mechanism of the calcium wave propagation is not clear (*e.g.*, secreted factors *vs.* gap junctional communication), studies to block gap junctional communication and/or paracrine signaling via ATP, nitric oxide, or prostaglandins would allow better characterization of the calcium signaling. Furthermore, exploration of the different mechanisms of calcium response, such as influx of external calcium or release of internal stores, in mechanically stimulated cells and those that received a transmitted calcium wave, would also be of interest. It would also be interesting to examine changes in calcium signal propagation with changes in cell connectivity, since osteoporotic bone has been shown to have decreased osteocyte connectivity. Since the activity of osteoblasts is known to be modulated by osteocytes (43), there may be modulation of calcium signal propagation between osteocytes and osteoblasts with alterations in osteocyte network connectivity and separation distances. Better understanding of signaling within osteocyte networks as well as between osteocyte networks and osteoblasts can provide information to devise treatments to enhance or manipulate bone adaptation.

Acknowledgement: This work is support by NIH grants AR048287, AR049613 and AR052417 (XEG), AR046568 (CTH), and the NSF CAREER award BES-0239138 (KDC). GMW, XJ and QX acknowledge NIH award GM065364. QX acknowledges support from NSF award PHY-0117795. This work is also supported by the Nanoscale Science and Engineering Initiative of the National Science Foundation under NSF Award Numbers CHE-0117752 and CHE-0641523, and by the New York State Office of Science, Technology, and Academic Research (NYSTAR).

References

1. Cowin, S. C. & Weinbaum, S. (1998) *Am J Med Sci*, **316**, 184-8.
2. Weinbaum, S., Cowin, S. C. & Zeng, Y. (1994) *J Biomech*, **27**, 339-60.
3. Vashishth, D., Verborgt, O., Divine, G., Schaffler, M. B. & Fyhrie, D. P. (2000) *Bone*, **26**, 375-80.
4. Cheng, B., Zhao, S., Luo, J., Sprague, E., Bonewald, L. F. & Jiang, J. X. (2001) *J Bone Miner Res*, **16**, 249-59.
5. Cheng, B., Kato, Y., Zhao, S., Luo, J., Sprague, E., Bonewald, L. F. & Jiang, J. X. (2001) *Endocrinology*, **142**, 3464-73.
6. Reilly, G. C., Haut, T. R., Yellowley, C. E., Donahue, H. J. & Jacobs, C. R. (2003) Biorheology, **40**, 591-603.
7. Yellowley, C. E., Li, Z., Zhou, Z., Jacobs, C. R. & Donahue, H. J. (2000) *J Bone Miner Res*, **15**, 209-17.
8. Knothe Tate, M. L., Adamson, J. R., Tami, A. E. & Bauer, T. W. (2004) *Int J Biochem Cell Biol*, **36**, 1-8.
9. Kufahl, R. H. & Saha, S. (1990) *J Biomech*, **23**, 171-80.
10. Moss, M. L. (1997) *Am J Orthod Dentofacial Orthop*, **112**, 221-6.
11. Reilly, G. C., Knapp, H. F., Stemmer, A., Niederer, P. & Knothe Tate, M. L. (2001) *Ann Biomed Eng*, **29**, 1074-81.
12. Ponik, S. M. & Pavalko, F. M. (2004) *J Appl Physiol*, **97**, 135-142.
13. Brock, A., Chang, E., Ho, C. C., LeDuc, P., Jiang, X., Whitesides, G. M. & Ingber, D. E. (2003) *Langmuir*, **19**, 1611-7.
14. Chen, C. S., Alonso, J. L., Ostuni, E., Whitesides, G. M. & Ingber, D. E. (2003) *Biochem Biophys Res Com*, **307**, 355-61.
15. Chen, C. S., Mrksich, M., Huang, S., Whitesides, G. M. & Ingber, D. E. (1998) *Biotechnol Prog*, **14**, 356-63.

16. Mrksich, M., Dike, L. E., Tien, J., Ingber, D. E. & Whitesides, G. M. (1997) *Exp Cell Res*, **235**, 305-13.

17. Singhvi, R., Kumar, A., Lopez, G. P., Stephanopoulos, G. N., Wang, D. I., Whitesides, G. M. & Ingber, D. E. (1994) *Science*, **264**, 696-8.

18. Healy, K. E., Thomas, C. H., Rezania, A., Kim, J. E., McKeown, P. J., Lom, B. & Hockberger, P. E. (1996) *Biomaterials*, **17**, 195-208.

19. Sorribas, H., Padeste, C. & Tiefenauer, L. (2002) *Biomaterials*, **23**, 893-900.

20. Prime, K. L. & Whitesides, G. M. (1991) *Science*, **252**, 1164-7.

21. Chen, C. S., Ostuni, E., Whitesides, G. M. & Ingber, D. E. (2000) *Methods Molec Bio*, **139**, 209-19.

22. Jiang, X., Ferrigno, R., Mrksich, M. & Whitesides, G. M. (2003) *J Am Chem Soc*, **125**, 2366-2367.

23. Love, J. C., Wolfe, D. B., Chabinyc, M. L., Paul, K. E. & Whitesides, G. M. (2002) *J Am Chem Soc*, **124**, 1576-7.

24. Hasenbein, M. E., Andersen, T. T. & Bizios, R. (2002) *Biomaterials*, **23**, 3937-42.

25. Feldkamp, L. A., Goldstein, S. A., Parfitt, A. M., Jesion, G. & Kleerekoper, M. (1989) *J Bone Miner Res*, **4**, 3-11.

26. Goldberg, G. S., Bechberger, J. F. & Naus, C. C. (1995) *Biotechniques*, **18**, 490-7.

27. Hantschel, T., Chow, E. M., Rudolph, D. & Fork, D. K. (2002) *Appl Phys Lett*, **81**, 3070-3072.

28. Hantschel, T., Chow, E. M., Rudolph, D. & Fork, D. K. (2003) *Microelectron Eng*, **67-68**, 803-809.

29. Chow, E. M., Chua, C., Hantschel, T., Van Schuylenbergh, K. & Fork, D. K. (2006) *IEEE Trans Components & Packaging Tech*, **29**, 796-803.

30. Donahue, S. W., Donahue, H. J. & Jacobs, C. R. (2003) *J Biomech*, **36**, 35-43.

31. Bailey, C. H. & Kandel, E. R. (1993) *Annu Rev Physiol*, **55**, 397-426.

32. Turner, C. H., Robling, A. G., Duncan, R. L. & Burr, D. B. (2002) *Calcif Tissue Int*, **70**, 435-42.

33. Bliss, T. V. & Gardner-Medwin, A. R. (1973) *J Physiol*, **232**, 357-74.

34. Hebb, D. O. (1949) in *The organization of behavior, a neuropsychological theory*, eds. (Wiley, New York).

35. Xia, S. L. & Ferrier, J. (1992) *Biochem Biophys Res Commun*, **186**, 1212-9.

36. Jorgensen, N. R., Geist, S. T., Civitelli, R. & Steinberg, T. H. (1997) *J Cell Biol* 1997 Oct, **139**, 497-506.

37. Romanello, M. & D'Andrea, P. (2001) *J Bone Miner Res*, **16**, 1465-76.

38. Hung, C. T., Pollack, S. R., Reilly, T. M. & Brighton, C. T. (1995) *Clin Orthop*, 256-69.

39. Tomkinson, A., Reeve, J., Shaw, R. W. & Noble, B. S. (1997) *J Clin Endocrinol Metab*, **82**, 3128-35.

40. Verborgt, O., Gibson, G. J. & Schaffler, M. B. (2000) *J Bone Miner Res*, **15**, 60-7.

41. Rubin, C. T., Bain, S. D. & McLeod, K. J. (1992) *Calcif Tissue Int*, **50**, 306-13.

42. Turner, C. H., Takano, Y. & Owan, I. (1995) *J Bone Miner Res*, **10**, 1544-9.

43. Takai, E., Mauck, R. L., Hung, C. T. & Guo, X. E. (2004) *J Bone Miner Res*, **19**, 1403-10.